Acta Neurochir (Wien) (2004) 146: 803–812
DOI 10.1007/s00701-004-0293-5

Acta Neurochirurgica
Printed in Austria

Review Article

Laser-induced thermotherapy of neoplastic lesions in the brain – underlying tissue alterations, MRI-monitoring and clinical applicability

P. C. Schulze[1], **H. E. Vitzthum**[2], **A. Goldammer**[2], **J. P. Schneider**[3], and **R. Schober**[4]

[1] Brigham and Women's Hospital, Cardiovascular Division, Department of Medicine, Harvard Medical School, Boston, U.S.A.
[2] University of Leipzig, Department of Neurosurgery, Leipzig, Germany
[3] University of Leipzig, Department of Radiology, Leipzig, Germany
[4] University of Leipzig, Department of Neuropathology, Leipzig, Germany

Published online June 7, 2004

Summary

Laser-induced thermotherapy (LITT) is a minimally invasive neurosurgical approach to the stereotactic treatment of brain tumors in poorly accessible regions. Its clinical applicability has been shown in several experimental and clinical studies under on-line monitoring by magnetic resonance imaging (MRI). This review characterizes LITT as an alternative neurosurgical approach with specific focus on the typical histological alterations and ultrastructural cellular changes following laser irradiation in the central nervous system. The spatial and temporal pattern of these changes is discussed in their relevance to the neurosurgical treatment of neoplastic lesions using LITT.

Keywords: Nd:YAG laser; brain tumor; histology; MRI.

Introduction

The surgical treatment of neoplastic lesions in poorly accessible regions of the central nervous system is still an unsolved problem. Minimally invasive techniques have been developed to reduce the side effects such as deterioration of functionally important regions of the brain. Laser-induced interstitial thermotherapy (LITT) as an approach to the treatment of brain tumors in stereotactic neurosurgery has shown its clinical applicability in experimental and clinical studies [4, 17, 30, 32]. Magnetic resonance imaging (MRI) serves as the most promising technique for on-line monitoring of LITT, and interventional imaging protocols have been developed in experimental studies and clinical trials [28, 30, 32]. LITT induces a circumscribed focal lesion in which parameters both in regard to the extent and the fate of the lesion have been described for various laser types [3, 25, 29]. The underlying laser-tissue interactions and resulting histological changes are well defined [25, 27, 29] and characterized as central coagulation necrosis and peripheral edema, subsequent resorptive changes and the formation of a rim of granulation tissue [25, 27, 29]. In this review, we will concentrate on alterations induced by the Nd:YAG-laser in brain tissue which have been extensively studied by our group.

Critically important for the treatment of brain tumors are both the primary tumor cell destruction and secondary alterations due to LITT on neoplastic cells [36]. The initial clinical outcome of patients after surgical treatment of brain tumors is mainly determined by the removal and destruction of neoplastic cells and a decrease in tumor size. However, marginal survival of tumor cells after treatment has been shown to be determining for the postoperative course. Secondary outgrowth of residual neoplastic cells may form the basis of a reformation of the tumor. Important for the prevention of tumor recurrences and, therefore, the outcome after surgical interventions are, in addition to the primary destruction of the solid tumor mass, alterations of the cell cycle and

cell life span that both are influenced by laser irradiation [27].

The development of LITT from an experimental technique to clinical applicability

First approaches to the treatment of brain tumors by thermal destruction of neoplastic tissue have been reported from ancient civilizations where the thermal energy of fire-heated instruments was used for the surgical treatments of neoplasms [7]. Initially, high-frequency coagulation of neoplastic lesions was used for the thermal destruction of tumor tissue. After continuous improvements in the underlying techniques since the early 1960s, Matthewson *et al*. first used LITT for the treatment of neoplastic liver lesions [20]. Experimental LITT using a Nd:YAG laser for the treatment of brain tumors was first described by Bown *et al*. in 1983 [6]. In those experiments, the laser energy was applicated interstitially using an optical fiber. Since then, a number of animal studies have investigated acute and chronic laser-tissue interactions in the brain, and histological studies revealed the laser-induced alterations of brain tissue on the cellular and subcellular level [25, 27, 29].

A relevant problem of LITT of the brain is the inhomogeneous tissue composition of the central nervous system [34, 35]. The laser-tissue interactions are mainly defined by optical properties of the tissue and resulting parameters of absorption and scattering. Optical properties of human brain tissues have been explored in a number of comparative studies [31, 39] and tissue-specific differences in absorption and scattering up to 300% were reported [9, 20, 35]. In addition, the optical properties of biological tissues change considerably due to coagulation-induced processes [31, 39].

The absence of an intraoperative monitoring and controlling of LITT inhibited its development into a clinically useful approach. Only after technical developments and the introduction of laser dosimetry [13], this still experimental technique became a therapeutic option attractive for further clinical verification. Furthermore, before LITT reached its clinical applicability, imaging techniques were developed for the intraoperative on-line monitoring of laser treatment. To date, magnetic resonance imaging (MRI) is the most advanced imaging technique for this purposes on the basis of a close relationship of changes in MRI signal and tissue temperature [15, 16] as well as the high tissue contrast of MRI in the brain [12]. These characteristics are now being used for the interventional imaging of laser-induced temperature changes within the tissue during therapeutic laser irradiation [17, 18, 32].

Altogether, these studies resulted in the establishment of protocols for the treatment of brain tumors using LITT evaluated in experimental animal studies [1, 28, 37, 38] and a number of clinical trials [4, 17, 23, 30].

Histological characterization of laser-tissue interactions in the brain

The acute and chronic tissue reaction after laser irradiation

Following laser irradiation, the laser lesion shows a typical architecture dependent on the interval following laser treatment [25]. The primary lesion exhibits differences in lesion diameter in dependence of the irradiation time and procedural energy deposition to the tissue but exhibits, in general, the typical architecture of a laser lesion that consists of a central coagulation necrosis, and a surrounding rim of edema adjacent to undamaged tissue (Fig. 1). Immediately after irradiation, the central zone of necrosis is not yet apparent but is demarcated by a rim of edema from the undamaged tissue. The necrosis becomes evident by a gradual loss of staining and early resorptive changes at their margins by day 3. A rim of granulation tissue is formed after one week and the edema spreads further to the periphery (Fig. 2). Finally, a cystic lesion results with variable remnants of unresorbed necrotic tissue and a mesenchymal and glial reaction at the margin remains. The immunohistochemical examination of tissue obtained from these lesions shows a distinct staining pattern in relation to the different zones of the lesion. Occasional nonspecific and diffuse immunostaining can be found in the central necrotic zone only [25, 27, 29].

Vascular effects of laser treatment

Following laser treatment, blood vessels generally appear engorged, containing leached erythrocytes that lay closely apposed to each other with a staining of their membranes only. The vascular tissue structure is well preserved after irradiation. Densely packed and decolorized red blood cells seem to be a characteristic histological marker of the intravascular laser effect [25]. The decoration of the lesion area by albumin, a serum-specific protein, indicates a breakdown of the blood-brain barrier [4, 25].

Vascular effects of laser treatment further include the thrombotic occlusion of vessels inside the central laser

lesion. These vascular structures within the necrosis are resorbed by invading mesenchymal cells during the course of regeneration. Vessels outside the margin of the laser lesion become the origin of outsprouting capillaries further invading into the lesion with functional importance for regenerative processes [27]. Also, these vessels clearly contain normal and undamaged erythrocytes 3 days after laser irradiation indicating a functional blood flow and the connection to the vascular tree [25, 27, 32].

Neuroaxonal alterations of LITT

The acute laser-induced destruction of brain tissue similarly affects neurons and axons leading to distinct histological alterations. Neuronal swelling, membranous defects with blurring of cell borders and reduced staining intensity are early signs of laser-induced tissue damage [25] accompanied by the neuronal expression of reactive proteins (Figs. 3 and 4). Under our experimental conditions, HSP 72 was the earliest stress marker detectable in damaged neurons following LITT (after 15 min). APP expression is typical for a delayed response accompanied by neurofilament 68 activation and APOE expression [25, 28]. When the central zone of necrosis becomes evident after one day, reactive changes can be found in damaged axons at the border zone. The axons initially show a distinct axonal swelling with "cork-screw"-like structures and outsprouting axons in radial orientation from the border to the center of the lesion [25, 29]. An accumulation of several reactive proteins (e.g. the amyloid precursor protein and neurofilament 68), as typical for regenerative changes of the brain, was found in these sprouts (Fig. 5). These changes can further be demonstrated using conventional staining methods like the Bodian stain (Fig. 6). In particular, the commissural system of the brain shows distinct axonal reactivity with highest staining intensity in damaged parts of the corpus callosum and the corpora striata adjacent to the laser lesion. However, axonal regenerative sprouts are of frustrane fate and resorbed with the initiation of mesenchymal transformation of the lesion resulting in a cystic defect [25, 28, 29].

Laser-induced alterations of glial cells

The specific appearance of a LITT lesion in the time course is mainly defined by resorptive changes and a reactive gliosis. Immunohistochemical staining for the glial fibrillary acidic protein (GFAP) clearly demonstrates astrocyte activation and the extent of gliosis. Increased numbers of GFAP-positive reactive astrocytes are present after one day already in the marginal zone, and the number of reactive astrocytes detected by GFAP increases thereafter. The marginal zone of the lesion shows a distinct three-layered structure. A zone of edema containing infiltrated granulocytes, lymphocytes and macrophages surrounds the central necrotic zone. A diffusely extending layer of GFAP-positive reactive astrocytes separates this zone of edema from the adjacent brain tissue that appears normal (Fig. 7). At the cellular level, different stages of astrocyte activation are detectable. One day following LITT, clumps of GFAP-positive cytoplasmatic material coat the nuclear membrane. After 3 days, GFAP staining appears in short cytoplasmatic processes. The intensity of GFAP immunoreactivity in reactive astrocytes that surround the necrotic zone increases until the end of the 2nd week. Later, sprouting capillaries and some GFAP-positive reactive astrocytes in addition to macrophages extend into the zone of necrosis. After 1 month, a layer of GFAP-positive astrocytes with centripetally decreasing density surrounds a cystic defect [29].

Fine structural analysis of membranes and cytoplasmatic alterations

The analysis of the acute and chronic changes following laser treatment consistently shows damage of cellular and subcellular membranes in the central zone surrounding the laser tip. Cell membranes and nuclear membranes of nerve cells, glial cells and endothelial cells either exhibit local defects or are broken up into fragments. In addition, subcellular membranes, in particular of mitochondria, display structural damage. Interestingly, curled fragments often form small vesicles. Vascular cells such as erythrocytes similarly show membrane defects leading to a loss of hemoglobin. Only basement membranes of capillaries and blood vessels seem to resist the laser treatment. In contrast, the investigation of the edema zone adjacent to the central necrosis displays no membrane ruptures [25].

These observations indicate that membrane alterations may play a leading role in the pathogenesis of laser-induced lesions. Several morphological observations may be explained by the generalized breakdown of cellular and subcellular membranes. Intravascular erythrolysis, a common phenomenon after laser irradiation, seems to be caused by a leakage of hemoglobin through defects in the cellular membranes of erythrocytes. The interstitial appearance of serum proteins such as albumin

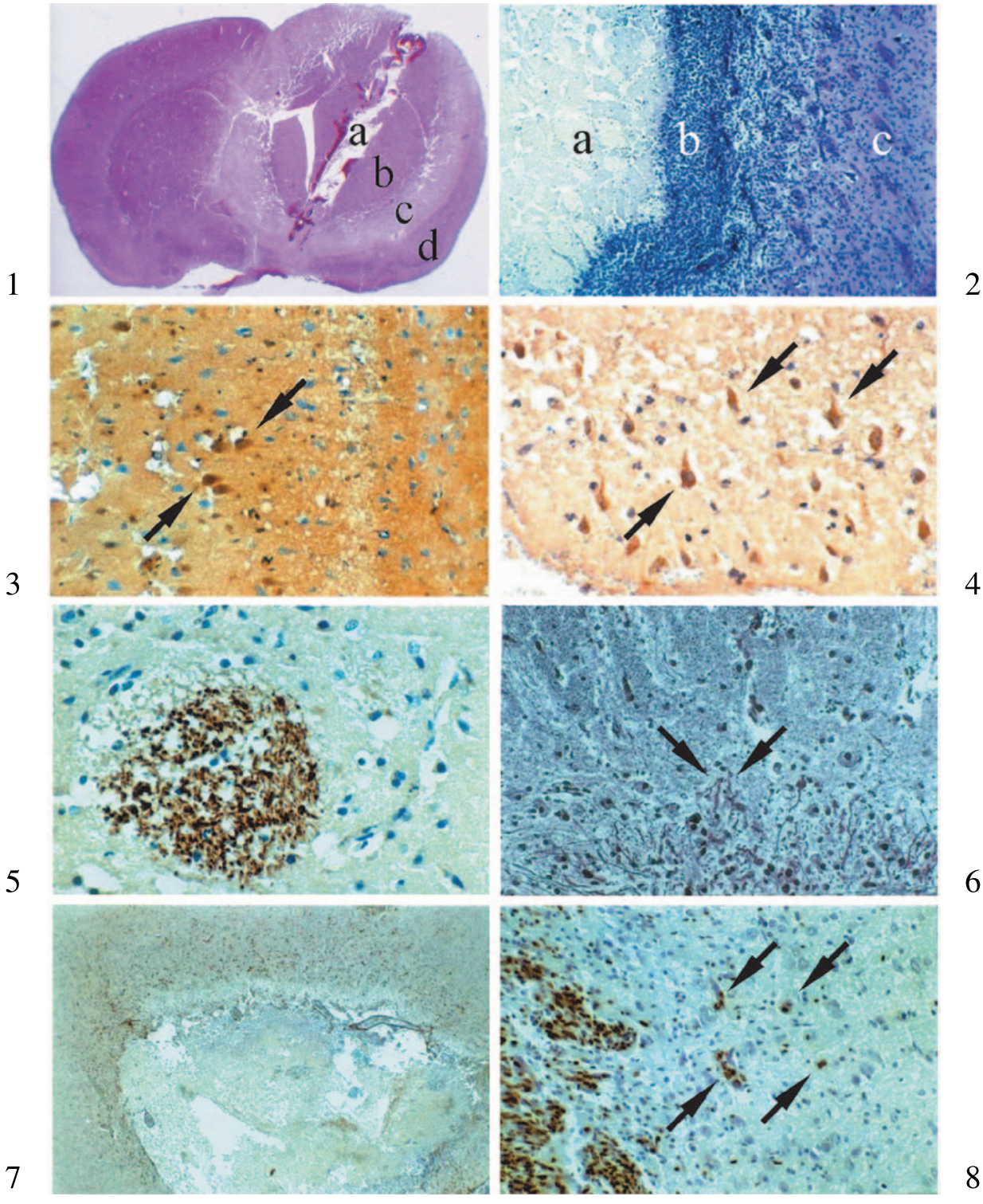

Fig. 1. Acute lesion of the brain following LITT with central laser probe defect (a) and coagulation necrosis (b) surrounded by perifocal edema (c) and normal tissue (d) (1 day post irradiation, ×10, H&E)

Fig. 2. Subacute LITT-lesion of the brain. The central zone of necrosis (a) is surrounded by a transitional zone of mesenchymal cells (b) adjacent to undamaged tissue (c) (1 week after LITT, ×65, H&E)

Fig. 3. Acute neuronal expression of HSP-72 following LITT (1 hour after LITT, ×65, anti-HSP-72)

which do not cross the blood-brain-barrier and typically are not detectable in the interstitium under normal conditions seems to be caused by membranous defects of the capillary endothelium [11, 25].

Alterations of neoplastic cells following laser irradiation

In several studies, no qualitative difference could be found in the general histological architecture of the LITT lesion in brain tumors and non-neoplastic tissues [4, 25, 27]. The zones of the lesion are clearly defined as central necrosis with a rim of edema. Interestingly, distinct changes can be seen in the size of the lesion in normal tissue in comparison to neoplastic tissue. This might be due to different histological and, therefore, optical properties of these tissues and a resulting difference in the sensitivity to laser energy defined by different neuroanatomical origin and ultrastructure as discussed below [39].

Surviving residuals of tumor cells start to grow further into the surrounding tissue as early as one day after LITT increasing the size of the neoplastic lesion. An outgrowth of tumor cells from the margin into the necrotic center of the lesion can also be detected (Fig. 8). Outsprouting capillaries from the edge of the lesion are surrounded by tumor cells that soon (after 3 days) form compact tumor cell masses. Interestingly, metastatic tumor masses in the necrotic areas show a higher grade of vascularisation than the primary tumor nodes before irradiation [27].

Laser-induced changes in optical properties of brain tissue

Published data on the optical properties of brain tissue are still rare. In recent studies, the optical properties of regional brain tissues before and after coagulation were investigated over a wide spectral range [31, 39]. These data show significant differences in optical properties of tissues from different regions of the brain [9, 31, 34, 39]. Also, coagulation-specific changes in absorption and scattering were investigated and a tissue-dependent but consistent increase in all investigated tissues was found. For white brain matter, absorption coefficients increase by a factor of 2 to 3 and scattering coefficients by a factor of two. For gray brain matter such as thalamus, both absorption and scattering coefficients increase nearly 3-fold, whereas for pons both interaction coefficients are approximately 4 times higher. The absorption coefficients of cerebellar tissue increase by a factor of 3 to 5, whereas the scattering coefficients were found to be twice higher than in untreated samples [39]. At present, the variation of these values cannot be explained on a fine structural basis alone, and gross structural differences such as intervening subarachnoid space as in the case of the cerebellar folia may also play a role. Similar changes of both absorption (by a factor of 2–10) and reduced scattering (by a factor of 2–4) coefficients in the wavelength range from 500 nm to 1100 nm were reported by other groups [5].

These findings do not allow a quantitative explanation of the thermally induced changes of tissue optical properties but it seems clear that such a significant increase of both interaction coefficients is the result of substantial structural changes. Histological analysis shows that coagulation causes essential brain tissue shrinkage, condensation as well as collagen swelling and homogenization of the vascular walls [25, 26]. Specific phenomena such as macroscopic shrinkage of brain tissue after coagulation depend on the structural tissue composition and are mainly determined by heat-induced loss of water by the brain tissue [39]. As a result, the concentration of chromophores and scattering inhomogenities increase and

Fig. 4. Reactive expression of APP in injured neurons (arrows) in distance from the laser lesion (1 day after LITT, ×120, anti-APP)

Fig. 5. Axonal accumulation of APP in LITT-damaged axons (24 after LITT, ×65, anti-APP)

Fig. 6. Regenerative sprouting of axons from the margin into the lesion (arrows) (3 days after LITT, ×65, Bodian stain)

Fig. 7. Reactive gliosis following LITT visualized by an increased expression of GFAP in activated astrocytes at the margin of the lesion (arrows) (1 day after LITT, ×8, anti-GFAP)

Fig. 8. Proliferating residual neoplastic cells (arrows) invading the necrotic lesion from the margin following LITT (1 week after LITT, ×65, anti-PCNA)

the tissues become optically denser leading to an essential increase of both scattering and absorption coefficients in the spectral range where water absorption is weak (up to 1100 nm–1300 nm). At the same time, tissue optical properties depend on differences in the quantitative distribution of several histological substructures such as the cytoplasmatic compounds (typical for gray matter such as thalamus with a high number of nerve cells) or axonal structures and myelin sheaths (typical for white matter with intercellular connections). Moreover, after coagulation, these compounds are changed specifically in response to heat-induced protein denaturation and homogenization, thus changing the optical properties of all cellular structures in regard to their thermal vulnerability.

MRI-based *on-line* monitoring of LITT

For exact and sensitive on-line monitoring of laser treatment, several MRI-based techniques have been developed [17, 37, 38]. With the fully awake patient in the MR unit, the evolving tumor destruction can be displayed during laser therapy using T_1-weighted gradient echo images [17]. After therapy, the typical appearance of laser-induced lesions in the brain has been described [30]. However, the use of T_1-weighted scans for monitoring of LITT results in several problems since changes of T_1 due to coagulation or necrosis and due to temperature elevation cannot be discriminated. On T_1-weighted images, the typical appearance of a laser-induced lesion consists of a central hyperintense zone that is surrounded by a hypointense peripheral zone [28]. Histopathological examinations support the assumption that signal intensity of the central zone is due to coagulation necrosis including hemoglobin decomposition products and of the peripheral zone due to perifocal edema [25]. During LITT, an additional decrease of signal intensity is related to the temperature-dependent prolongation of the T_1-relaxation time. This results in a blurring of the borders of the lesion and consequently in difficulties to precisely define the size of the damaged zone. To overcome this problem, MRI-based temperature quantification was proposed [12, 17]. This implicates the assumption that specific temperatures can be correlated with distinct histopathological pattern and the border of the histologically damaged zone correlates with certain temperatures [28].

For MRI-based thermometry, several temperature sensitive MRI-parameters have been used. T_1-relaxation time maps based on a multi-point Turbo-FLASH sequence showed a linear correlation between temperatures and T_1-relaxation times [18] that, however, is strongly tissue dependent. Furthermore, during laser experiments large deviations of the calculated temperatures from measured temperatures were observed [18]. In contrast, the proton-resonance-frequency-method for temperature quantification [8, 14] is mainly tissue-independent (with the exception of adipose tissue) [12]. Using this method, color-coded MRI-temperature maps can be correlated to the histological findings in laser-irradiated brain tissue, and the border of the central region with irreversible tissue damage was defined at the 60 °C isotherm [28].

Clinical applicability of LITT for the treatment of brain tumors

Interstitial thermotherapy by stereotactic laser irradiation as an alternative approach in the therapy of brain tumors has been investigated in clinical trials by several groups [2, 10, 17, 19, 22, 24]. Technical prerequisites are a Nd:YAG-laser that is exactly adjustable in the low power range (3–5 W/s), transmission systems suitable for stereotactic applications and a fiber tip that allows circumferential and homogenous irradiation of the tissue over long exposure times (up to 30 min) [13, 25]. As discussed above, intraoperative temperature-sensitive monitoring by MRI in real time mode can reliably be used for therapeutic evaluation of laser treatment. Using values from databases of optical characteristics of human brain tissue and brain tumors, an exact treatment planning and dosimetry is possible and can closely be adjusted to the treatment-dependent changes in penetration depth and absorption maxima [32, 39].

On interventional MRI, the acute laser-induced lesion appears as a central hyperdense area [17]. The size of the lesion is influenced by the histological structure of the tissue under treatment and the resulting optical properties. In addition, thermal convection by blood vessels might play a role in modulating the lesion size [19]. During the procedure, conversation with the patient and continuous proof of neurological function is possible. The main intraoperative side effect of interstitial laser irradiation is mild neurological deterioration of the fully awake patient [17, 19]. An increase in lesion size in the first week post-surgery has been described by several groups [17, 19]. It is attributed to the developing perifocal edema and further cytotoxic processes in the area surrounding the lesion. However, after one week, the lesion starts to shrink in an exponential pattern with

a half-life period of 10 weeks [30]. The final cystic lesion shows decreased signal intensity at the margin on MRI most probably due to hemosiderin deposition [30].

Treatment of neoplastic lesions of the brain using LITT – single center experiences

A total of 15 patients (mean age: 59.3 years) with an intracranial supratentorial tumor of the cerebrum was biopsied and treated in a 0.5 Tesla superconducting MR system "SIGNA SP/i" (GE Medical Systems, Milwaukee, Wis) between 1996 to 2001. The Ethics Committee of the University of Leipzig had approved the experimental protocol. All patients underwent laser-induced thermotherapy (LITT). After positioning of the anaesthetized patient and attachment of the flex coil in the open MR, localization of the tumor was determined by MRI imaging. T2 weighted Fast Spin Echo (FSE) and T1 weighted Spin Echo (SE) sequences were followed by a near real time imaging using a T1 weighted continuous Fast Multiplanar Spoiled Gradient Echo (FMSPGR) sequence controlled by the "Flashpoint Position Encoder" (Image Guided Technologies, Bolder, Co) with three light-emitting diodes (LED) [21, 22, 33]. This allows an interactive selection of axial, coronal, sagittal or oblique T1-weighted images. In cases of known enhancing lesions, Gd-DTPA (Magnevist, Schering, Berlin, Germany) was administered (0.1 mmol/kg body weight). The virtual axis for biopsies including the planned surgical approach and definition of the optimal site of craniotomy was determined to get a three-dimensional imagination of the planned cannula in relation to anatomic structures and the pathological lesion. The biopsy trajectory was chosen in order to avoid structures of risk whenever possible.

Following skin incision, a standardized burr hole with a vertical bone wall and a suitable size for fixing the NEUROGATE® (Daum, Schwerin, Germany) after dura incision is realized using a special broach. Using this fixation device during surgery, the placement of the biopsy cannula or laser fibre sheath can be changed at any time supported by the LED-tracking system and MRI guidance. After biopsy and histological analysis of tissue specimens, the light guide (Dornier, Germering, Germany) covered by a sheath (Somatex, Germany) for further minimal invasive treatment was inserted under MRI guidance [33]. During the laser therapy, energy was applied using a 12 W pulsed laser for a treatment time of 10–16 min. Using the on-line monitoring of LITT, the treatment modalities were adjusted to the temperature within the lesion and the size of the tumor and its neighboring structures. The heating process was monitored by a continuous gradient echo sequence to detect proton resonance frequency shift. A special processing software (RTIP, GE Medical Systems, Milwaukee, Wis) enables an interactive monitoring of temperature courses thus allowing on-line evaluation of the procedure and immediate adjustment of therapy if necessary [33].

Table 1. *Neuropathological diagnoses of neoplastic lesions*

	n = 15
Glial tumor	
– Astrocytic	
Grade IV	5
Grade III	3
Nonglial tumor	
– Metastatic	7

All 15 patients (8 female, 7 male) were examined stereotactically and treated by LITT without intraoperative complications. All target lesions could be detected by open MR and were punctured successfully. Based on histopathological assessment, MRI and clinical characteristics, a diagnosis was established in all cases. The histological diagnosis obtained from brain biopsy included eight cases (53.3%) of high-grade glioma (glioblastoma: 5/8, anaplastic astrocytoma: 3/8) and 7 cases (46.7%) of metastatic tumors (Table 1). Mean time interval between initiation and end of anesthesia was 296.1 min (Min: 130, Max: 350 min). Total time of the stereotactic interstitial laser procedure was 224.6 min (Min: 105, Max: 330 min).

LITT of a right temporal glioma – an illustrative case report

A 79-year-old female patient had a history of headache and nausea for 3 years, which was associated with generalized tonic-clonic seizures. Cranial computed tomography (CCT) and magnetic resonance imaging (MRI) showed a right temporal lesion with a central and ring-enhancement and a profound white matter edema (Fig. 9a, b). Because of the patients age and the reduced physical conditions a biopsy and LITT was suggested. Preoperative planning of the procedure was carried out and image-guided surgery in the open MR started. The intraoperative temperature monitoring using an open MRI unit (0.5 T) is based on a spoiled GE sequence (TE 27 ms, TR 59 ms, TA 8 s, SD 10 mm,

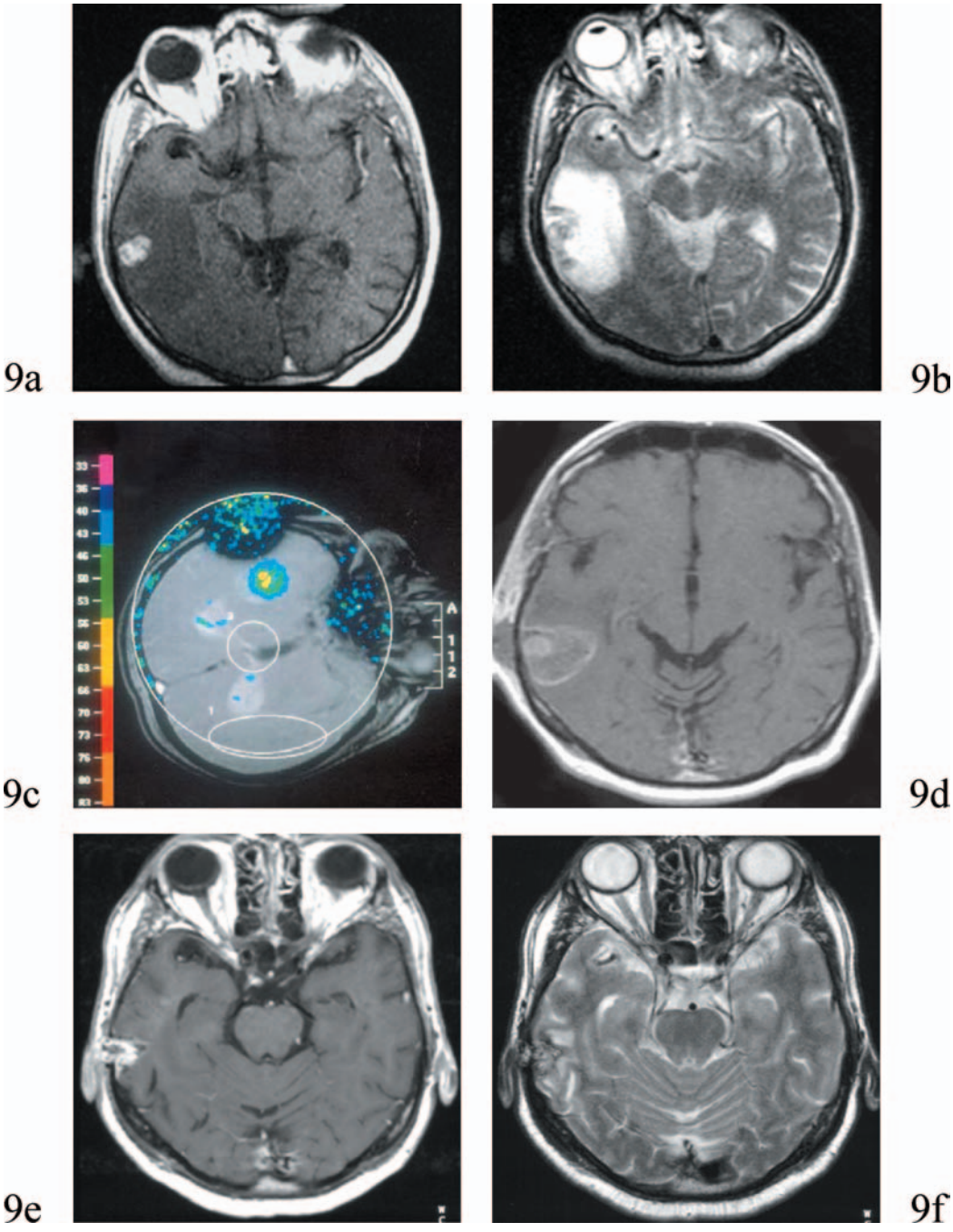

Fig. 9 a–f. LITT for the clinical treatment of a right temporal glioblastoma (confirmed by histological assessment of intraoperative biopsy). Preoperative MRI scan demonstrating an enhancing lesion with surrounding edema (a). On-line monitoring of intraoperative temperature distribution during experimental LITT by MRI using the temperature-sensitive proton-resonance-frequency-method (b). Interstitial temperature distribution is visualized by color-coded isothermes (software RTIP, GE Medical Systems, Milwaukee, Wis) surrounding the laser tip (c). One week following LITT, the lesion has decreased in size and is surrounded by a hyperintense enhancing rim of perifocal edema (d). Two month following LITT, the size of the lesion is reduced and appears as a central cystic lesion surrounded by remnants of unresorbed necrotic tissue as well as a mesenchymal and glial reaction at the margin (e). In addition, the edema has significantly shrinked in size (f)

matrix 256×256), which displays temperature-dependent changes in proton resonance frequencies by phase contrast. For this purpose, a representative section of the tumor was selected and a high resolution background image chosen from which changes in temperature distribution were visualized by phase contrast after acquisition of a baseline image. A specific software (Real Time Image Processing, RTIP, GE Medical Systems,

Milwaukee, Wis) was used for the continuous assessment of interstitial temperature distribution which was monitored on-line on the MRI console (SPARC 20, Sun, Mountain View, CA, USA). After burr hole trepanation and fixation of the NEUROGATE®, insertion of a side cut biopsy cannula (Daum, Schwerin, Germany) was realized. The procedure was guided by interactive MR imaging. Biopsies were taken from different areas of the tumor after fixation of the biopsy cannula. Intraoperative histological diagnosis revealed an anaplastic astrocytoma (WHO grade III). LITT was performed using a Nd:YAG laser (Medilas, Germering, Germany) and interstitial thermotherapy light guide (Dornier, Germering, Germany) with continuous temperature-sensitive MR imaging (Fig. 9c). At the end of the procedure, MRI was performed to exclude surgery-associated complications and to visualize immediate therapeutic effects (Fig. 9d). The postoperative course was uneventful. No postoperative radiotherapy was applied. The patient recovered well and no negative side effects of the procedure were observed. The follow-up examination by MRI after two weeks showed a significantly reduced tumor volume surrounded by a perifocal edema, which disappeared completely two months after surgery (Fig. 9e, f).

Conclusion

In conclusion, LITT is a suitable minimally invasive technique for the treatment of brain tumors in poorly accessible regions but can also be applied for superficially located tumors. The resulting laser-induced lesions of the brain show a typical architecture with central necrosis surrounded by a rim of edema and result in a cystic defect after resorptive and regenerative changes. Effects of laser irradiation include cellular membrane rupture and fragmentation of subcellular components in addition to heat-induced tissue damage. A significant problem of LITT is the survival of neoplastic cells at the margin of the lesion leading to secondary tumor growth following treatment. Further developments in on-line imaging techniques as well as additional intra- or postoperative measures directed to surviving tumor cells are necessary to overcome this problem and improve the outcome of patients after LITT.

LITT represents an alternative palliative therapeutic option in patients with malignant intracerebral tumors determined by histology. It might be particularly useful for the treatment of older patients in reduced physical condition and of compact tumors in inaccessible regions of the brain. However, a definitive comparison of LITT with conventional neurosurgical techniques is currently difficult due to inhomogenous patient groups and the lack of standardized treatment plans for LITT. Several studies showed the clinical applicability of LITT in neurosurgery but randomized clinical trials comparing LITT to other neurosurgical approaches are pending and data on long-term outcome of patients after LITT are still lacking.

References

1. Anzai Y, Lufkin RB, Hirschowitz S, Farahani K, Castro DJ (1992) MR imaging-histopathologic correlation of thermal injuries induced with interstitial Nd:YAG laser irradiation in the chronic model. J Magn Res Imaging 2: 671–678
2. Ascher PW, Justich E, Schrötter O (1991) Interstitial thermotherapy of central brain tumors with the Nd:YAG laser under real-time monitoring by MRI. J Clin Laser Med Surg 9: 79–83
3. Berlien H-P, Mueller G (2001) Angewandte Lasermedizin. Ecomed, Berlin, 2001
4. Bettag M, Ulrich F, Schober R, Sabel M, Kahn T, Bock WJ (1992) Laser-induced interstitial thermotherapy in malignant gliomas. Adv Neurosurg 22: 253–257
5. Black JF, Barton JK, Frangineas G, Pummer H (2001) Cooperative phenomena in two-pulse two-color laser photocoagulation of cutaneous blood vessels. SPIE 4244: 12–24
6. Bown SG (1983) Phototherapy of tumors. World J Surg 7: 700–709
7. Breasted JH (1931) The Edwin Smith surgical papyrus. University of Chicago
8. De Poorter J, Nagter CD, Thompson C, Stahlberg F, Achten E (1994) The proton-resonance-frequency-shift-method compared with molecular diffusion for quantitative measurement of two-dimensional time-dependent temperature distribution in a phantom. J Magn Res Imaging 103: 234–241
9. Eggert HR (1985) Optical properties of brain tissue and brain tumors at the wavelength of the Nd-YAG laser (lambda = 1060). Adv Neurosurg 13: 276–281
10. Fan M, Ascher PW, Schrötter O, Ebner F, Germann RH, Kleinert R (1992) Interstitial 1.06 Nd:YAG laser thermotherapy for brain tumors under real-time monitoring of MRI: Experimental study and phase I clinical trial. J Clin Laser Med Surg 10: 355–361
11. Gutknecht N, Kanehl S, Moritz A, Mittermayer C, Lampert F (1998) Effects of Nd:YAG-laser irradiation on monolayer cell cultures. Lasers Surg Med 22: 30–36
12. Harth T, Kahn T, Rassek M, Schwabe B, Schwarzmaier HJ, Lewin JS, Mödder U (1997) Determination of laser-induced temperature distributions using echo-shifted Turbo FLASH. Magn Reson Med 38: 238–245
13. Hessel S (1990) Technical prerequesites for the interstitial thermotherapy with the Nd:YAG laser. Lasermed 1: 36–40
14. Ishihara Y, Calderon A, Watanabe H, Okamoto K, Suzuki Y, Kuroda K, Suzuki Y (1995) A precise and fast temperature mapping using water proton chemical shift. J Magn Res Med 34: 814–823
15. Jako GJ, Jolesz FA (1986) The control of Nd:YAG laser fiber optics hyperthermia with magnetic resonance imaging. SPIE 712: 72–77
16. Jolesz FA, Bleier AR, Jakob P, Ruenzel PW, Huttl K, Jakob G (1988) MR imaging of laser-tissue interactions. Radiology 168: 249–253
17. Kahn T, Bettag M, Ulrich F, Schwarzmaier HJ, Schober R, Fürst G, Mödder U (1994) MRI-guided laser-induced interstitial

thermotherapy of cerebral neoplasms. J Comput Assist Tomogr 18: 519–532
18. Kahn T, Harth T, Schwabe B, Schwarzmaier HJ, Mödder U (1997) MRI temperature quantification at 1.5 T in vitro: comparison of fast T_1-maps and a phase-sensitive sequence. Fortschr Rontgenstr 167: 187–193
19. Leonardi MA, Lumenta CB, Gumprecht HK, Einsiedel GHV, Wilhelm T (2001) Stereotactic guided laser-induced interstitial thermotherapy (SLITT) in gliomas with intraoperative morphologic monitoring in an open MR-unit. Minim Invas Neurosurg 44: 37–42
20. Matthewson K, Coleridge-Smith A, Northfield TC, Bown SG (1986) Comparison of continuous-wave and pulsed excitation for interstitial Neodymium-YAG laser induced hyperthermia. Las Med Sci 1: 197–201
21. Menovsky T, Beek JF, van Gemert MJ, Roux FX, Bown SG (1996) Interstitial laser thermotherapy in neurosurgery: a review. Acta Neurochir (Wien) 138: 1019–1026
22. Roux FJ, Devaux B, Mordon S, Nguyen S, Chodkiewicz JP (1990) The use of 1.32 Nd:YAG laser in neurosurgery: Experimental data and clinical experience from 70 patients. J Clin Laser Med Surg 8: 55–61
23. Roux FX, Merienne L, Leriche B (1992) Laser interstitial thermotherapy in stereotactical neurosurgery. Las Med Sci 7: 121–126
24. Sakai T, Fujishima I, Sugiyama K, Ryu H, Uemura K (1992) Interstitial laserthermia in neurosurgery. J Clin Laser Med Surg 10: 37–41
25. Schober R, Bettag M, Sabel M, Ulrich F, Hessel S (1993) Fine structure of zonal changes in experimental Nd:YAG laser-induced interstitial hyperthermia. Lasers Surg Med 13: 234–241
26. Schober R, Ulrich F, Sauder T, Dürselen H, Hessel S (1986) Laser-induced alteration of collagen substructure allows microsurgical tissue welding. Science 232: 1421–1422
27. Schulze PC, Adams V, Busert C, Bettag M, Kahn T, Schober R (2002) Effects of laser-induced thermotherapy (LITT) on proliferation and apoptosis of glioma cells in rat brain transplantation tumors. Lasers Surg Med 30: 227–232
28. Schulze PC, Kahn T, Harth T, Schwarzmaier HJ, Schober R, Schulze CP (1998) Correlation of neuropathologic findings and phase-based MRI temperature maps in experimental laser-induced interstitial thermotherapy. J Magn Reson Imaging 8: 115–120
29. Schulze PC, Thal DR, Bettag M, Schober R (1998) Brain tissue damage and regeneration monitored by β-amyloid precursor protein in experimental laser-induced interstitial thermotherapy. Neuropathology 18: 55–61
30. Schwabe B, Kahn T, Harth T, Ulrich F, Schwarzmaier HJ (1997) Laser-induced thermal lesions in the human brain: short- and long-term appearance on MRI. J Comput Assist Tomogr 21: 818–825
31. Schwarzmaier HJ, Yaroslavsky A, Yaroslavsky I, Goldbach T, Kahn T, Ulrich F, Schulze PC, Schober R (1997) Optical properties of native and coagulated human brain structures. SPIE 2970: 492–499
32. Schwarzmaier HJ, Yaroslavsky I, Yaroslavsky A, Fiedler V, Ulrich F, Kahn T (1998) Treatment planning for MRI-guided laser-induced interstitial thermotherapy of brain tumors – the role of blood perfusion. JMRI 8: 121–127
33. Stollberger R, Ascher PW, Huber D, Renhart W, Radner H, Ebner F (1998) Temperature monitoring of interstitial thermal tissue coagulation using MR phase images. J Magn Res Imaging 8: 188–196
34. Svaasand LO, Ellingsen R (1983) Optical properties of human brain. Photochem Photobiol 38: 293–299
35. Svaasand LO, Ellingsen R (1985) Optical penetration in human intracranial tumors. Photochem Photobiol 41: 73–76
36. Terzis AJ, Dietze A, Bjerkvig R, Arnold H (1997) Effects of photodynamic therapy on glioma spheroids. Br J Neurosurg 11: 196–205
37. Tracz RA, Wyman DR, Little PB (1992) Magnetic resonance imaging of interstitial laser photocoagulation in the brain. Lasers Surg Med 12: 165–173
38. Tracz RA, Wyman DR, Little PB (1993) Comparison of magnetic resonance images and histopathological findings of lesions induced by interstitial laser photocoagulation in the brain. Lasers Surg Med 13: 45–54
39. Yaroslavsky AN, Schulze PC, Yaroslavsky IV, Schober R, Ulrich F, Schwarzmaier HJ (2002) Optical properties of selected native and coagulated human brain tissues in vitro in the visible and near infrared spectral range. Phys Med Biol 47: 2059–2073

Comment

The presented work represents a review describing in detail the Laser-induced thermotherapy technique (LITT) as a neurosurgical approach to the stereotactic treatment of brain tumours in poorly accessible regions.

This is a well written comprehensive review on the LITT approach for the treatment of brain tumours. The manuscript adequately describes the LITT technique and its biological effects on normal brain and malignant tissue.

R. Bjerkvig
Bergen

Correspondence: Ralf Schober, M.D., Selbständige Abteilung für Neuropathologie, Institut für Pathologie, Universitätsklinikum Leipzig, Liebigstraße 26, 04103 Leipzig, Germany. e-mail: neuropath@ medizin.uni-leipzig.de